8

Numerical Simulations of Microscale Gas Flows: Continuum Approach

A. Chaudhuri†, A. Hadjadj†, C. Guha‡ and T. K. Dutta‡
†*CORIA-UMR CNRS 6614, Avenue de l'Université, 76801 St Etienne du Rouvray France*
‡*Chemical Engineering Department, Jadavpur University, Kolkata-700032 India*

1. Introduction

Enormous technical applications of micro and nanosciences have evolved as one of the most active interdisciplinary field of research and development during last two decades. The journey of scientific innovations in micro and nanoscale has just begun and yet plenty of rooms at the bottom remain to be explored. It is the imagination and vision of Nobel Laureate, Professor Richard Feynman that have been implemented in the field of micro and nanodevices. Micro and nanodevices can be widely used in aerospace, automotive, biotechnology, medicine, instrumentation, robotics manufacturing and many other applications. In coming decades, Micro-Electro-Mechanical-Systems (MEMS)/Nano-Electro Mechanical-Systems (NEMS) technology are going to become part of our daily life. MEMS refer to devices that have typical characteristic lengths lying between 1 μm and 1 mm that combine electrical and mechanical components. In this chapter, we will restrict our discussion to only microscale gas flows in continuum regime together with the application of wall-slip models and numerical methods that are commonly used in this field. The dynamics of fluids and their interaction with surfaces in microsystems are very much different from those in large-scale systems. In microsystems, the flow becomes granular for liquids and rarefied for gases, and the walls tend to move. Phenomena such as viscous heating, thermal creep, electro-kinetics, anomalous diffusion, and even quantum and chemical effects appear important. Design and optimization of effective micro and nanodevices require a deeper physical understanding of hydrodynamic and kinetic phenomena in single and multiphase flows in small dimensions. The material of the wall, the quality of the surface as well as the energy exchange in small dimensions play the crucial roles for microscale flow characteristics. Since surface to volume ratio of microstructures is very high surface effects dominate over volumetric effects. The local Knudsen number is a measure of the degree of rarefaction of gases encountered in MEMS devices. The popular methods for analyzing the fluid-flow and heat transfer characteristics of gases in microscale include the particulate method of Boltzmann equations, Direct Solution Monte Carlo (DSMC) and Burnett equation models. Several investigators have used the DSMC approach where the Knudsen number is very high involving high

computation cost and time requirement. The standard continuum approach of considering the bulk of the fluid with no-slip wall conditions can no longer predict the momentum and heat transfer accurately in microdevices. Navier-Stokes simulations of gas flow in microdevices with wall-slip models have evolved as an alternative solution technique to treat this miniaturization effect in the slip flow regime.
In section 2, we will briefly highlight the governing equations of fluid-flow with slip models and the applicability of the continuum approach. The following sections will provide the discussion on simulations of non-reactive and reactive compressible flows in microscale. In section 3, we will present the behavior of non-reactive fluid-flow and heat transfer in microchannels followed by the comparison of fluid-flow behavior in micronozzles and the conventional full-scale nozzles. The effect of miniaturization on flow separation pattern will also be addressed in this section. In section 4, we will illustrate few reactive flow studies in microchannels. Keeping in view the useful application of shock waves at microscale we will demonstrate the studies of shock-wave attenuation in microchannels in section 5. Finally, the results will be summarized in section 6 and concluding remarks will be provided as the basis of future work in this area.

2. Flow Regimes and Models

Knudsen number is defined as the ratio of microscopic length scales (mean free path) and characteristic length of the physical domain. This is the key factor determining the gas flow regimes. The effect of miniaturization in microscale gas flows can be attributed to rarefaction, giving rise to strong analogy between low-pressure flows and microscale flows. Based on the ratio of Mach number and Reynolds number, the Knudsen number can also be interpreted as

$$Kn = \sqrt{\gamma\pi/2}\,\frac{M}{\mathrm{Re}} \tag{1}$$

where γ is the ratio of specific heats. Equation (1) relates rarefaction effects to compressibility and viscous effects through Mach and Reynolds numbers respectively. As Knudsen number increases, the rarefaction effects become more and more pronounced and eventually the continuum assumption breaks down. Traditionally, gas flows are divided into four regimes as i) $Kn \le 10^{-3}$: continuum regime, ii) $10^{-3} < Kn \le 10^{-1}$: slip regime, iii) $10^{1} < Kn \le 10$: transitional and iv) $Kn > 10$: free-molecular regimes.
The effect of wall in microdimension is of utmost importance which plays crucial role in microscale gas flows affecting the momentum and energy transfer. Classical continuum regime is essentially governed by compressible Navier-Stokes equations with conventional boundary conditions. On the other hand, in slip flow regime, Knudsen layer (zone of non-equilibrium near the wall) must be taken into account with modified velocity slip and temperature jump at the wall. The continuum approach is thus applicable taking sufficient precautions using appropriate slip models. Most of the Microsystems using gases as working fluid fall in slip flow regime or early transition regime (M. Gad-el-Hak, 1999; Karniadakis & Beskok, 2002). Solution of Navier-Stokes equations with wall-slip models thus evolved as relatively cheaper choice compared to DSMC and Burnett equation models in terms of computational costs and complexity.

Compressible Navier-Stokes system of equations with Newtonian stress tensor, Fourier law of thermal diffusion, Fick's law of mass diffusion and calorically perfect/thermally perfect gas/ gas-mixture behavior are usually assumed as governing equations for defining compressible fluid flow. The validity of these assumptions is widely accepted and has been addressed by many authors in standard books and literature. Specifically, in the following section, we wish to emphasize on the modified slip boundary conditions applicable in accordance with the continuum approach.

2.1 Wall-Slip Models

In microscale gas-flows, the interaction of the fluid molecules with the surface material (chemical affinity) plays an important role. Momentum and energy transfer can thus be correlated to the interaction of impinging gas molecules to the surface of the wall material. On the basis of kinetic theory, Maxwell postulated and proved the existence of wall-slip. In order to formulate the velocity slip, Maxwell considered details of momentum transfer mechanism of the molecules and the wall, introducing TMAC (Tangential Momentum Accommodation Coefficient, σ_v). This lies between zero (no momentum transfer to the wall) and unity (gas molecules transmit entire tangential momentum to the wall) representing specular and diffusive reflection. Later Smoluchowski in 1898 experimentally confirmed the hypothesis of Poisson to define the temperature jump corresponding to velocity slip at the wall containing thermal accommodation coefficient σ_T. Detail discussions about accommodation coefficients have been reported in Gad-el-Hak, (1999); Karniadakis, (2000) and Arkilic et al., (2001). In most of the numerical simulations, it is usual practice to set accommodation coefficients to unity. It is really a tremendous challenge to get the desired accuracy to measure the precise mass flux experimentally with imposed pressure gradients. Arkilic et al., (2001) experimentally determined sub-unity TMACs for nitrogen, argon and carbon dioxide in contact with single-crystal silicon. Ewart et al., (2007) reported their recent experimental determination of TMAC based on mass flow measurements. Based on findings of Porodonov et al., (1974); Arkilic et al., (1997b); Maurer et al., (2003); Colin et al., (2004) and Ewart et al., (2007), it can be summarized that TMAC lies between 0.81-0.981 for nitrogen, 0.7-0.942 for argon and 0.895-0.986 for helium. Suitable sub-unity values of the TMAC thus can be utilized in numerical simulations. Maxwell's first order velocity slip with thermal creep and corresponding temperature jump relation can be written as:

$$u_{slip} - u_{wall} = \frac{2-\sigma_v}{\sigma_v}\lambda\left.\frac{\partial u}{\partial n}\right|_w + \frac{3}{4}\frac{\mu}{\rho T}\left.\frac{\partial T}{\partial s}\right|_w \tag{2}$$

$$T_{slip} - T_{wall} = \frac{2-\sigma_T}{\sigma_T}\frac{2\gamma}{(\gamma+1)}\frac{k}{\mu C_p}\lambda\left.\frac{\partial T}{\partial n}\right|_w \tag{3}$$

where n and s denote the normal and tangential directions of the derivative terms. λ, u, μ, ρ, T, k and C_p are mean free-path, velocity, viscosity, density, temperature, thermal conductivity and specific heat at constant pressure, respectively.

Significant discrepancies have been observed between experimental data and DSMC calculations based on first order slip models, for Knudsen number greater than 0.1. Several authors have proposed higher-order boundary conditions to extend the validity of the slip-flow regime. In non-dimensional form, the generalized second-order slip velocity relation (Sreekanth, 1969) can be expressed as:

$$\hat{u}_{slip} - \hat{u}_{wall} = \xi_1 Kn \left.\frac{\partial \hat{u}}{\partial \hat{n}}\right|_w + \xi_2 Kn^2 \left.\frac{\partial^2 \hat{u}}{\partial \hat{n}^2}\right|_w \quad (4)$$

The tabulated coefficients ξ_i, used by various researchers for the above general equation, are reported in Colin, (2005). Nevertheless, the implementation of higher-order boundary conditions of this form is particularly difficult. The recent work of Dongari et al., (2007) has dealt with analytical solution of Navier–Stokes equations using second-order slip model for isothermal gas flow in long microchannel. The change in curvature of pressure versus the streamwise direction has been reported and the presence of Knudsen's minima has also been correctly predicted by their developed theory.

In recent studies, implementation of the first-order slip boundary conditions on various reacting and non-reacting test-cases has been carried out after the successful validation of the developed explicit Navier-Stokes solver. We have utilized robust shock capturing schemes including AUSM (Advection Upwind Splitting Methods, Liou & Steffen, 1993) and subsequent modified version of these schemes as well as high-order WENO (Weighted-Essentially Non-Oscillatory) schemes (Jiang & Shu, 1996) for convective flux calculations and central differencing discretization of diffusive fluxes. Usually, choice of shock capturing schemes is essential to deal with flow discontinuities over a wide range of Mach number. Detail of these schemes is well known to computational community and widely available in literature. In this chapter, we will mainly focus on the physics of the microscale thermal-fluid behavior setting aside the details of the numerical tools.

3. Fluid Flow and Heat Transfer in Microchannels and Micronozzles

3.1 Microchannels

Microchannels are currently being used in many areas such as those of medicine, biotechnology, avionics, telecommunications, metrology, computer technology, office equipment, home appliances, environment protection etc. Experimental investigations of flow and heat transfer through microchannels of various cross sectional geometries have been carried out by many researchers, (Wu & Little, 1984; Pafler et al., 1990; Choi et al., 1991; Pong et al., 1994; Liu et al., 1995; Harley et al., 1995; Yu et al., 1995; Shih et al., 1996; Bayt & Breuer, 1998), mainly by focusing on the measurements of pressure drop and bulk fluid temperatures at the channel ends. Numerous discrepancies have been encountered compared to the macroscale behavior. In the review of Papautsky et al., (2001), it is reported that the data of the slip-flow gas indicate an approximate 60% reduction in friction factor compared to macroscale theory for a single-phase laminar flow. Rostami et al., (2002) made a detail review of the aforementioned experimental findings along with the numerical findings of Beskok et al., (1996); Arkilic et al., (1997) and several other contributors. For microchannels and microtubes, Reynolds analogy and Colburn analogy were found invalid

(Wu & Little, 1984; Choi et al., 1991). Relatively recent experimental work of Celata et al., (2007) reported the determination of local friction factor (tube diameters ranging from 30 - 254 μm) for helium taking compressibility effects into account. Their findings are in close agreement with incompressible and quasi-incompressible correlations. The existence of nonlinear pressure drop across the channel for higher-Knudsen number flows and dependency of product of friction factor and Reynolds number for fully developed laminar flow on Reynolds number have been reported in various experimental studies. Application of first-order slip models to account for the non-continuum effects evolved as favorable choice by the numerical findings of the literature. Chen, (2004) utilized 3D numerical simulation to predict the steady compressible laminar flow in microchannel and reported that the slip effect reduces the wall friction and curvature of the pressure distribution. Later, Jain & Lin, (2006) also emphasized about the need of accounting 3D effects for the prediction of friction coefficients in microchannels.

Arkilic et al., (1997a) reported a theoretical model for slip flow in long isothermal channels. The corresponding nonlinear pressure distribution (normalized by outlet pressure) along streamwise direction (normalized by the length of the channel) is given by

$$\hat{P}(\eta) = -\chi + \sqrt{\chi^2 + (1+2\chi)\eta + (\Pi^2 + 2\chi\Pi)(1-\eta)} \tag{5}$$

where

$$\chi = 6\frac{2-\sigma_v}{\sigma_v} Kn_o \tag{6}$$

In the above equation, Π is the ratio of inlet and outlet pressure and Kn_o is the outlet Knudsen number.

We carried out a standard benchmark test of isothermal slip flow through microchannel for validation of first-order slip model using finite volume method (FVM). The dimension and other flow-field parameters are shown in Figure 3.1.1a, where nitrogen gas is being considered as the working fluid. It can be seen from Figure 3.1.1b that the agreement between the FVM and analytical solution (Arkilic et al., 1994) is excellent. Computational results are also in good agreement with experimental data of Pong et al., (1994).

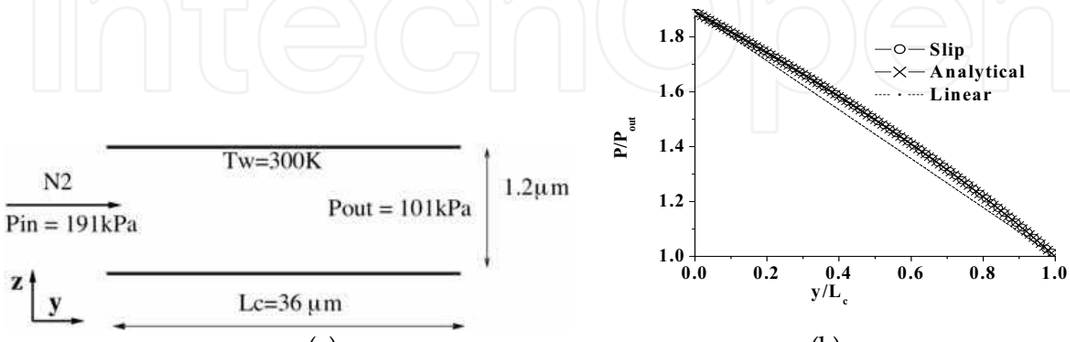

(a) (b)

Fig. 3.1.1. Validation of first-order slip model: (a) problem description, (b) pressure profile

The study of microchannel flow is partly in response to the need of thermal control in the operation of MEMS. Yan & Farouk, (2002) investigated high Knudsen number low-speed flow through partially heated parallel plates using DSMC. Chaudhuri et al., (2007b) studied the effects of Knudsen number and gas species at atmospheric pressure levels using similar configuration for partially heated microchannel (resembling classical Graetz problem). The dominant molecular diffusion and nonlinear pressure distribution for higher Knudsen number are found to be similar for both rarefied (Yan and Farouk, 2002) and microscale behavior.

In comparison to experimental and numerical studies of subsonic flow inside microchannels, studies on flow-thermal characteristics in high-speed flows are not abundantly found in literature. Liou & Fang, (2001) reported that the magnitude of the temperature jump at the wall increases with increasing Knudsen number. The heat transfer at the isothermal wall is found to increase significantly with Knudsen number. Raju & Roy, (2005) investigated the heat transfer characteristics of high-speed compressible flows and compared DSMC results of Liou & Fang, (2001) with their finite element simulations. Chaudhuri et al., (2007a) compared finite volume simulation with results of the DSMC (Liou & Fang, 2001; Le & Hassan, 2006) and FEM results (Raju & Roy, 2005) for inlet Mach number 4.15. Acceptable agreement has been achieved in terms of detached bow shock patterns and flow field inside the microchannel (Figure 3.1.2). Chaudhuri et al. further extended hypothetical test-cases with higher inlet Mach number (hypersonic). The jump in near wall temperature appeared higher for higher inlet Mach numbers (Figure 3.1.2). Position of fully developed thermal boundary-layer shifted further downstream with increasing inlet Mach number.

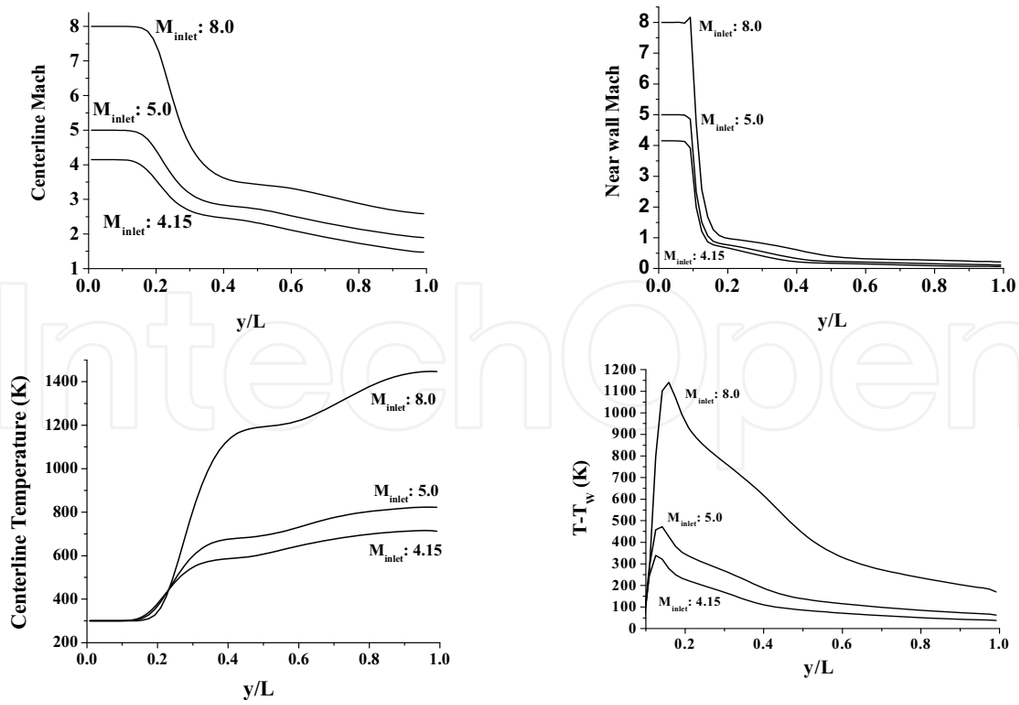

Fig. 3.1.2. Comparison of Mach number and temperature distribution (streamwise) for high-speed gas flow through microchannels with inlet Knudsen number 0.062.

3.2 Micronozzles

Variety of aerospace missions and application systems have been benefited from micro-engineering technology due to reduced size, mass and power requirements (Janson et al., 1999). Among them, micropropulsion devices provide an active field of applied research. Electrical and chemical microthrusters are developing in recent years in order to fulfil the required design and fabrication of microspacecraft with high accuracy. The main application of the microthruster is the micropropulsion system for microsatellites weighing typically 20 to 100 kg or nanosatellites typically less than 20 kg. Among the propulsion systems which use MEMS technology or hybrid technology for the miniaturization are the cold gas thrusters, the subliming solid thrusters, the field emission electric propulsion (FEEP), or the hall-effect thrusters. Unique thrust requirements have initiated the need for optimal design and fabrication concept for a MEMS-based microthruster. Due to the inherent complexity of the fluid dynamics in the micrometer scale, experimental and numerical studies were proposed for better understanding of the flow properties and optimal design (Kujawa et al., 2003). The performance of a micropropulsion system is primarily determined by the performance of micronozzles. The nozzle converts the stored energy in a pressurized gas into kinetic energy through an expansion. The nozzle efficiency is characterized by the amount of kinetic energy leaving the nozzle, and is governed by the exit Mach number. Many experimental and numerical studies were carried out on microthruster/micronozzle behavior for varying geometries and propellants. Bayt et al., (1997) experimentally and numerically studied a micron scale Laval nozzle. For the numerical study, they used a 2-D finite volume NS solver. Bayt, (1999) fabricated an extruded 2-D converging-diverging nozzle with minimum throat widths averaging 19 μm and 35 μm etched by deep reactive ion-etching. Their experiment reveals that supersonic flow can be achieved in contoured micronozzles (outlet Mach number 3.8 for expansion nozzle ratio of 17) for micropropulsion systems. Reed, (2003) carried out experiments on planar micronozzles for nitrogen and helium flows under ambient temperature to study the nozzle performance with different exit to throat aspect ratios. Lewis, (2000) dealt with design and fabrication of initial prototypes of microthruster chips. From relatively more recent work of Chen et al., (2005), it can be realized that thrust is not only a function of pressure difference but also depends on the flow history for miniature nozzles. In spite of existence of discrepancies on thrust and mass flow measurements among the theoretical and experimental findings the following points can be summarized for mini/microscale nozzle behavior (Rossi et al., 2000; Rossi et al., 2001; Hammel, 2002; Alexeenko et al., 2002; Hao et al., 2005; Liu et al., 2006; Moríñigo et al., 2007; Xu & Zhao, 2007; Lin & Gadepalli, 2008). (1) Applicability of slip models in DSMC/NS solutions is valid in slip flow regimes for successful prediction of micronozzle flow behavior. (2) Precise low thrust in the order of mN to μN can be produced for micropropulsion systems. (3) There exists shock free supersonic flow in the diverging section compared to conventional nozzle under similar constraints. In addition, the sonic point usually appears further downstream of the throat location. (4) Flow-separation with high expansion ratio decreases with decreasing the nozzle size.

In our previous work (Chaudhuri et al., 2006), numerical results for flow through microthruster are compared with the 1-D numerical study by Rossi et al. (2000), and 2D FEM results by Raju & Roy, (2002) as a no-slip benchmark problem predicting essential 2-D features of the fluid-flow inside the micronozzle. In this section, we will present three test-cases with different outlet pressure (65 kPa, 55, kPa and 10 kPa) to investigate the internal

micronozzle flow having the same inlet pressure of 100 kPa. Figure 3.2.1 shows the schematic of the nozzle configuration. The effect of the nozzle size with different scales is also studied for outlet pressure of 10 kPa. It can be seen from Figure 3.2.2 that the flow inside the micronozzle remains entirely subsonic for outlet pressure 65 kPa. When the outlet pressure is kept 55 kPa, (Fig 3.2.2) the first sonic point appears further downstream of the throat. The existence of the shock free supersonic zone with gradual dissipation to subsonic flow is also predicted by the simulation and is similar to the findings of Hao et al., (2005). On the other hand, the fully supersonic flow is observed downstream of the throat (Figure 3.2.3) for outlet pressure of 10 kPa.

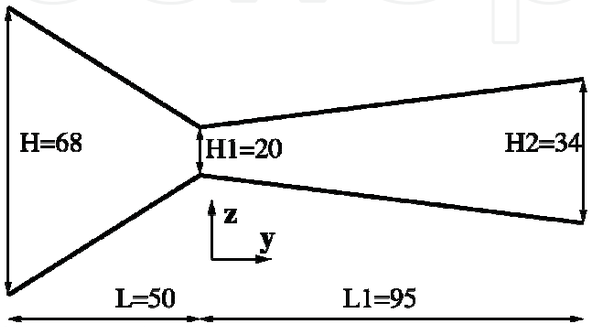

Fig. 3.2.1 Schematic of micronozzle, dimensions are in μm

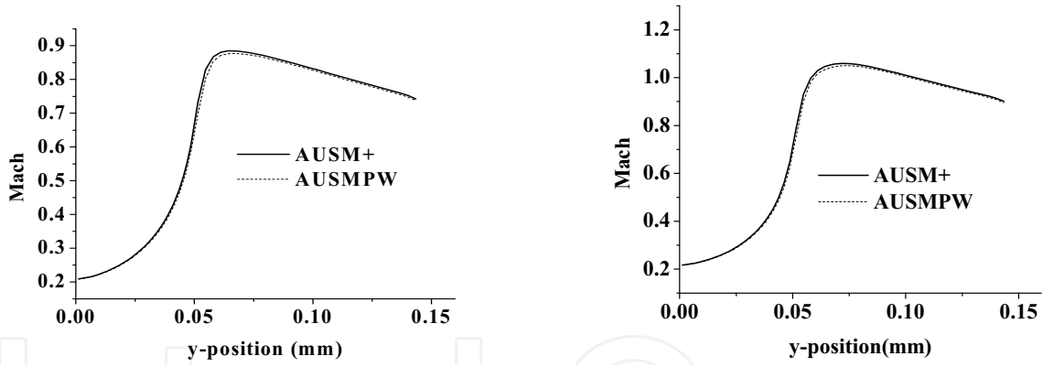

Fig. 3.2.2. Centreline Mach distribution, case: 65kPa (left), case: 55kPa (right)

The dominant surface-to-volume ratio effect drastically changes the flow field in microscale compared to the normal-scale nozzles. Hao et al., (2005) reported the presence of shock wave in a larger nozzle (1000 times). The higher temperature at the throat is correlated to the lower value of the Mach number at the micronozzle throat (Hao et al., 2005). It is evident from Figure 3.2.2 that both AUSM+ and AUSMPW predict the essential flow characteristics with similar level of accuracy. Figure 3.2.3 illustrates the effect of size on the micronozzle flow. Five different micronozzles with throat dimension 4 μm, 8 μm, 20 μm, 100 μm and 200 μm are further studied in this work (varying scales with geometrical similarity). The outlet Mach number increases with the increase of nozzle scale and the position of sonic point moves away from the throat towards the outlet of the nozzle with the decrease in size of the micronozzle. The predicted exit Mach numbers with no-slip condition are 2.02, 1.91, 1.57, 1.2

and 1.001 for nozzle throat sizes of 200 μm, 100 μm, 20 μm, 8 μm and 4 μm respectively. Hao et al., (2005) measured pressures at two different positions near the throat of the micronozzle having 20 μm throat dimension. The Knudsen number for 65 kPa, 55 kPa and 10 kPa in this dimension marginally falls in the slip flow regime. The results are in good agreement with experimental data of Hao et al., (2005). From Figure 3.2.4, it can be seen that while decreasing the dimension of nozzle throat, the deviation between the two solutions (with and without slip boundary conditions) becomes more and more prominent. This is in accordance with the increase in Knudsen number varying from 0.002 to 0.034 in smaller dimensions. Recent numerical investigations of San et al., (2009) on the same configuration revealed similar results which is in accordance with the above presented findings.

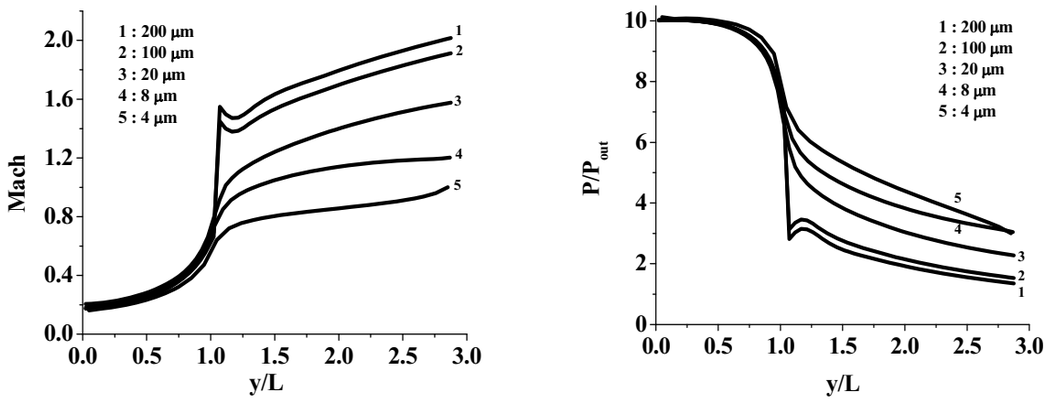

Fig. 3.2.3. Comparison of centreline Mach distribution (left), centreline non-dimensional pressure distribution (right) case: 10 kPa with varying scale of the nozzle by AUSM+

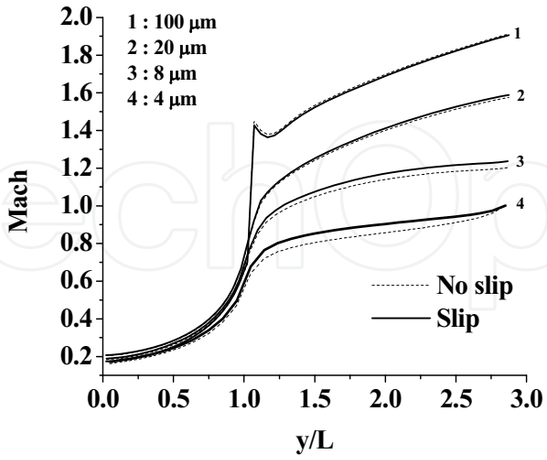

Fig. 3.2.4. Comparison of slip/no-slip conditions, Case: 10 kPa by AUSM+

3.3 Flow Separation in Microscale

In previous sub-sections, we have discussed thermal flow characteristics in straight microchannels and subsequently, the behavior of micronozzles with variable cross sectional areas. It can be noted that often bends or curvatures are unavoidable in microsystems. Studies of flow separation and related heat-loss in microscale are thus in need of more experimental measurements as well as numerical predictions to quantify the physics of the phenomena. Studies of thermal microflow with bends, cavities and separation flows over backward-facing steps as well as in micro-mixing systems are important for microfluidic devices. Literatures regarding these areas are inadequate till now. Microchannels with three different bend configurations (integrated with pressure sensors) have been fabricated and characterized by Lee et al., (2001). Their measurements of both mass-flow rate and pressure reveal that secondary flows can exist in microchannels with miter-bends, whereas fully attached flow occurs for curved and double turn bends. Yu et al., (2005) studied experimentally several microchannels (of l-2 μm height) with cavities. They concluded that fully attached flow occurs for low Reynolds number similar to microchannel flows with fewer cavities. Rawool et al., (2005) studied numerically flow through microchannels with obstructions placed along the channels walls. They reported that recirculation zones are created downstream of these obstructions and the skin friction increases nonlinearly with the increase in obstruction height and decreases nonlinearly with the increase in Reynolds number. Xue & Chen, (2003) conducted numerical simulations of backward-facing step flows for various Knudsen numbers from the slip to transition flow regimes. It has been shown that flow separation, recirculation, and reattachment disappear for Knudsen number greater than 0.1. The movements of molecule with mean free paths larger than the backward-facing step dominate the flow behavior.

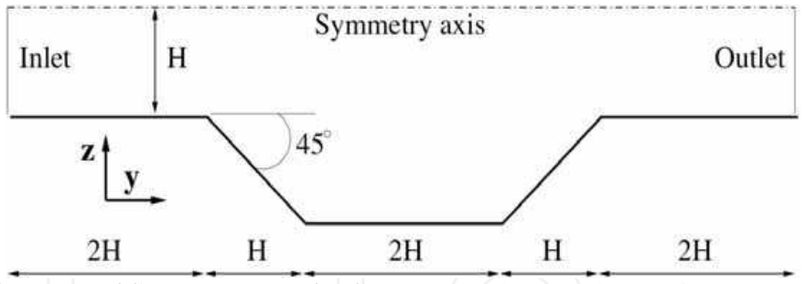

Fig. 3.3.1. Schematic of flow geometry for flow-separation at microscale

Chaudhuri et al., (2008) studied numerically the pressure driven flow through trapezoidal cavity configuration and confirmed the effect of miniaturization on gas flow-separation. Figure 3.3.1 shows the schematic of the flow geometry taken for this study (pressure driven air flow with ratio of inlet to outlet pressure equals to 1.26). Results for three test cases (case 1: H=5 μm, case 2: H=0.5 μm and case 3: H=50 μm) have been presented for demonstration. It can be seen, from Figure 3.3.2, that under similar conditions, flow separation does not occur for case 2 (highest Knudsen number) and flow remains fully attached. On the other hand, flow-separation appears most pronounced for case 3 with largest dimension while case 1 shows intermediate behavior. As expected, effect of slip conditions has been found negligible for case 3.

4. Reactive Flow in Microchannels

Microcombustors, microburners and microactuators, for instance, are the critical power components in MEMS devices. Many experimental techniques, developed for macroscale combustion devices, cannot be directly applied to study microcombustion due to the miniaturization effect. Micropower systems for application in portable electronics, microsensors, and other platforms are often the limiting components in terms of both size and performance. Many micropower systems require a high-temperature reservoir in the form of a combustor. Usually microcombustors can be categorized as (1) homogeneous gas-phase combustors and (2) heterogeneous catalytic combustors. Gas-phase microcombustors are limited by residence time constraints that can be quantified in terms of the Damköhler number. Performance of catalytic microcombustors is typically limited by diffusion of fuel species to the active surface as governed by the Peclet number. Miniaturization of the conventional reactor incurs high thermal losses and radical depletion on the wall which significantly affect the combustion behavior. Two of the most prominent questions are related to the lower limit of the combustor size and the combustion efficiency. Flow distributions of the reaction mixture are also very important factors for microreactor performance. Depending on geometry, composition, and flow rate, methane/air flames are typically quenched for dimensions less than 1–2 mm (Davy, 1817; Maekawa, 1975; Ono & Wakuri, 1977; Fukuda et al., 1981; Lewis & von Elbe, 1987; Linan & Williams, 1993). Although flame propagation at microscale is feasible, the interplay of kinetics and transport in flame stability and combustion characteristics of these systems are not yet well understood (Norton & Vlachos, 2003). In microscale, combustion can be advantageous due to possible faster ignition leading to reduced NOx production.

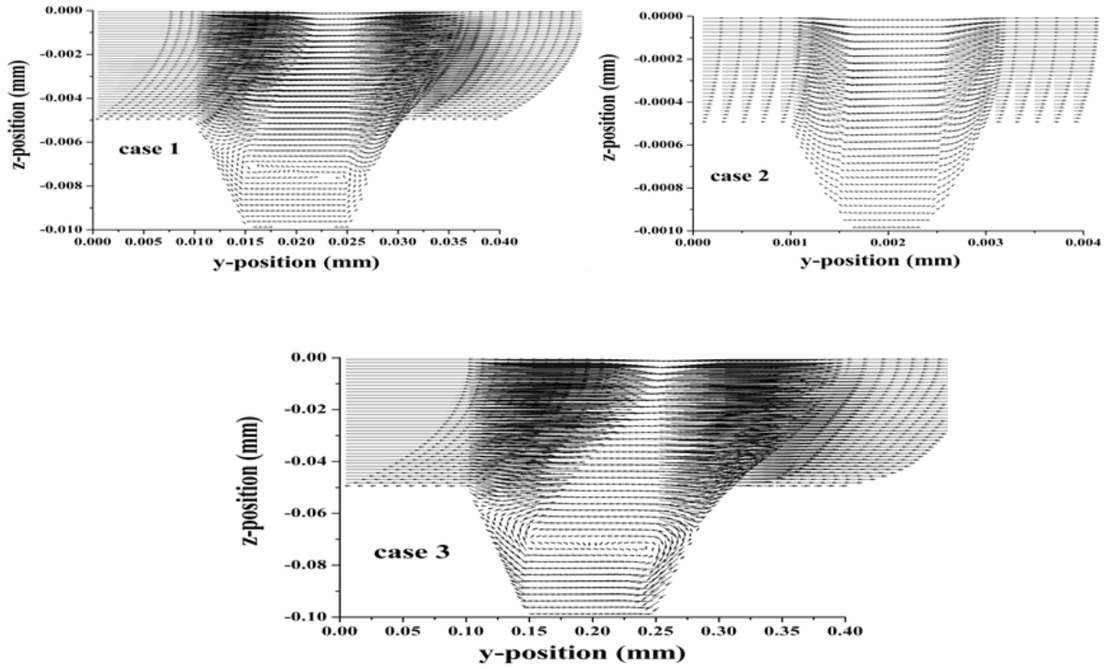

Fig. 3.3.2. Velocity vector plot for different test cases

Size constraint enhances the difficulty of systematic experimental investigations in microreactors. Undoubtedly, numerical simulations are indispensable for studying flow in microcombustors. Lee & Kwon, (2002) developed a theoretical model to simulate the flame propagation with non-negligible heat-loss to the wall in a closed vessel (chamber height ranging from 0.61 to 3.0 mm). Preheating or higher initial pressure of the combustible mixture of gases inside the combustor were found to be capable of increasing the combustion efficiency as well as the thermal efficiency of a power device. Many studies on the characterisation of microflames and stability flame regimes have been reported in the literature (Norton & Vlachos, 2003; Norton & Vlachos, 2004; Miesse et al., 2004; Li et al., 2005a; Yuasa et al., 2005; Shaurya et al. 2007). Federici & Vlachos, (2008) studied the stability of a premixed C3H8/air microflame in a heat recirculation reactor (HRR) and compared it with a single-channel microcombustor. In their scale analysis, Li et al., (2004) reported a relation between the hydrogen flame-temperature in a laminar microcombustor (radii of 3, 4 and 6 mm) and the external wall surface temperature where detailed reaction mechanisms were involved. Leach et al. (2006) presented an analytical model for the prediction of heat-exchange effects within the structure of a micro-channel combustor, and heat-loss from the structure to the environment. Yang et al., (2002) tested different cylindrical microcombustors (2–3 mm diameter). The designed combustors of 2-3 mm diameter with backward facing step were found to be very effective in controlling the position of the flame and widening the range of operation based on the inlet flow velocity as well as H2/air ratio. Later, Li et al., (2005b) investigated the effects of step height and external wall temperature on the structure of hydrogen–air flame. Numerical results showed that the external wall temperature increases drastically with decreasing the step height keeping unchanged the axial flame temperature.

Understanding the behavior of flame propagation with deflagration-to-detonation transition (DDT) in microchannels is typically important for the design of micropropulsion and micro power systems. Ott et al., (2003) predicted mechanism of laminar flame acceleration of air-acetylene system in narrow channel. Gamezo & Oran, (2006) extended the work of flame acceleration to micropropulsion application. Chaudhuri et al., (2007d) studied the phenomenon of flame acceleration of premixed combustible air-acetylene mixture towards the open end of an adiabatic microchannel by solving Navier-Stokes (NS) system of equations with single-step chemistry model. The length (L: y axis) and height (H: z axis) of the 2-D microchannel are 1cm and 600 μm respectively with left-end closed and right-end open. The flame has been initiated by a planar discontinuity in temperature and density located at 366 μm from the closed end. Burned and unburned gases are specified on the left and the right of the discontinuity respectively. The chemical reactions of air-acetylene mixture are considered using a single-step first-order kinetic model similar to that of Ott et al., (2003); Gamezo & Oran, (2006). The initial conditions and other physical and chemical parameters taken are similar to those presented in (Ott et al., 2003; Gamezo & Oran, 2006). Owing to the symmetry of the physical domain, only half of the domain has been simulated. Symmetry and adiabatic wall conditions are applied accordingly. The position of the flame is defined as the location where the flame-front reaches the temperature of 1000K. Figure 4.1 depicts flame positions near the wall as well as at the centreline. It is evident from Figure 4.2 that the centerline flame velocity increases with time while reaching the end of the microchannel. Also, as shown in Figure 4.3, the transverse velocity component increases at the end of the microchannel as the flow evolves. The maximum outflow velocity reaches ≈

138 m/s. Figure 4.4 shows the product mass fraction and streamwise velocity contours respectively at 0.000195s. The boundary layer growth and burning of boundary layer material clearly reveal the phenomenon of flame acceleration in microchannel. Gamezo & Oran, (2006) concluded that the maximum flame acceleration occurs when the channel height (640 μm) is about five times larger than the reaction zone of a laminar flame. Flame acceleration in microchannel close to this aspect ratio has been studied. The developed solver is capable of predicting the mechanism of flame acceleration, flame propagation and maximum outflow velocities. Results are in good agreement with the conclusion drawn by Gamezo & Oran, (2006) related to the maximum flame acceleration configuration of the adiabatic microchannel.

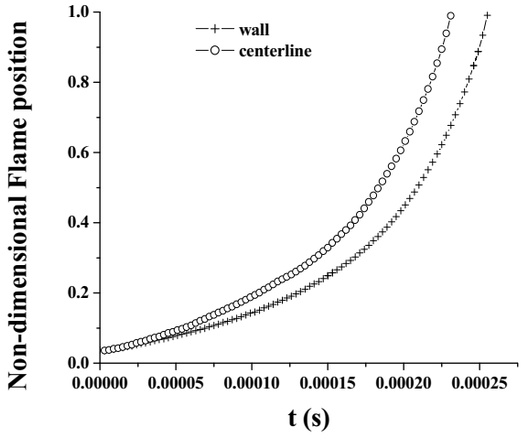

Fig. 4.1 Time evolution of flame position

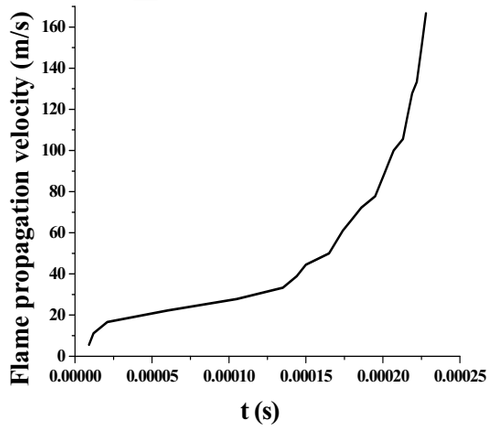

Fig. 4.2 Flame propagation velocity

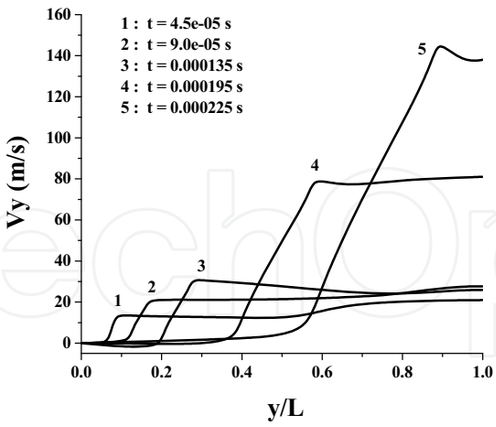

Fig. 4.3 Time snaps of the centerline streamwise velocity component

A detailed review on the application of micro-structured reactors for heterogeneous catalyzed gaseous phase reactions has been presented by Kolb & Hessel, (2004). Lee et al., (2002) proposed the concept of a MEMS scale reciprocating device powered by burnt gas and fabricated its prototype to investigate the applicability of the concept in a microscale

power generator. Maruta et al., (2002) studied the extinction limits of self-sustaining methane-fueled combustion on platinum catalyst in non-adiabatic microscale flow reactor channels. Boyarko et al., (2005) experimentally studied fuel rich gaseous hydrogen and oxygen on catalytically active surfaces within 0.4 and 0.8 mm internal diameter microtubes. Good agreement with a plug flow model prediction of detailed gas-phase chemistry and surface kinetics has been reported. Schwarz et al., (2009) showed that microstructured reactors are well suited for application in strongly exothermic heterogeneous catalyzed gaseous phase reactions since they involve isothermal reactions over a wide range of concentrations and temperatures. Xu & Ju, (2004) developed a slip model for species to consider the rarefied gas effect at the boundary in microscale reactors and nanoscale structures. However, no further supporting studies are available for this slip model.

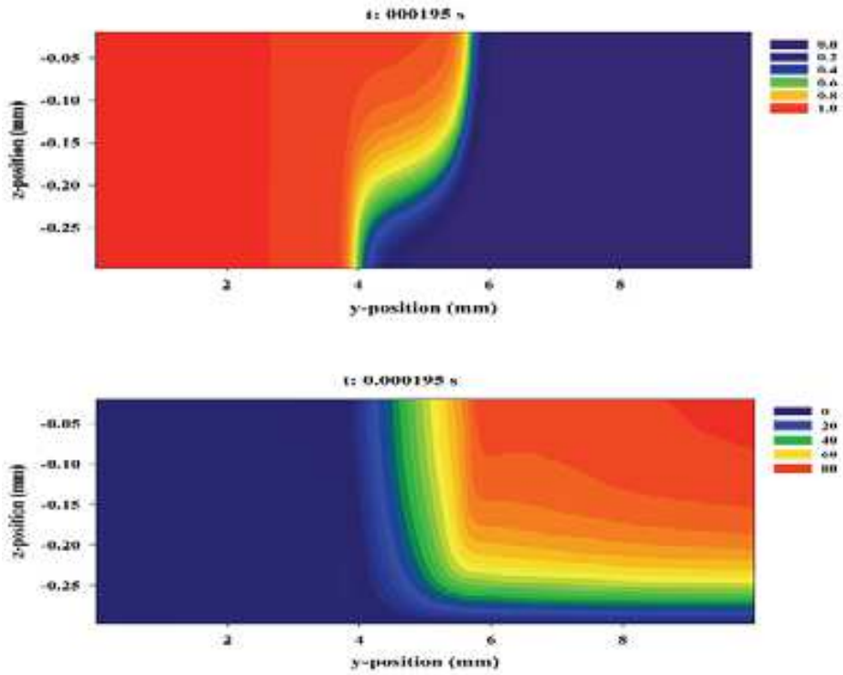

Fig. 4.4 Product mass fraction contour (top) and velocity contour (bottom) at t: 0.000195 sec

Apart from the studies of flame characteristics in microdimensions, viscous and diffusion effects on the propagation of supersonic combustion waves in microchannels have yet to be studied and understood. Kivotides, (2007) analysed the propagation of detonation waves in channels of height 10 μm to illustrate the viscous effects on detonation characteristics. Motivated by our previous studies of strong heat release in high-speed microchannel flows, the possibilities of reacting flows at microscale have been further investigated (Chaudhuri et al., 2007c). For this purpose, a stoichiometric air-acetylene mixture is considered at hypersonic speed (M=8) in three different microchannels having 10 mm length and different heights (60 μm, 80 μm 200 μm for cases 1, 2 and 3, respectively). The inlet velocity for each case is taken as uniform with a constant temperature of 300 K and atmospheric pressure. All variables are obtained as a part of the solution at the outlet boundary and all variables are specified at the inlet boundary for each test case. Inlet conditions are assigned as the initial

conditions for all variables throughout the computational domain. The chemical reactions of air-acetylene mixture are approximated as single-step first-order simple kinetics (similar to flame acceleration study). The effects of channel aspect ratio and wall temperature have been carefully investigated. Figure 4.5 illustrates the mass fraction of the combustible mixture, and temperature contours for case 1. It is clear from Figure 4.5 that the air-acetylene mixture gets completely burned inside the channel. The reaction zone initiating from the wall region meets at the centerline forming a bent structure of discontinuity. The double hill formation due to heat released by combustion in the burned region of the temperature contour is also evident from Figure 4.5. The high wall-friction associated with the microscale flow brings about the initiation of combustion near the wall region which, in turn, produces the complex discontinuity of Mach and temperature contours. The contour plots of the individual variables for case 2 & 3 are shown in Figs. 4.6 & 4.7. The height-to-length ratios (H/L) of the microchannel are gradually increased. It is clearly evident that with the increase in H/L, the zone of burned gas moves towards the right hand side (RHS) of the microchannel. For highest H/L, the reacted burned gas zone remains detached near the centerline. It can be clearly observed, from Figure 4.8, that the point of initiation of combustion from the wall and corresponding centerline distribution of mass fraction of combustible mixture gradually shifts towards the RHS of the microchannel from case 1 to case 3. The rise in temperature near the wall due to wall friction initiates the chemical reaction of the combustible mixture close to the wall region and the reacted zone reaches the centerline for smaller height-to-length ratio of the microchannels. The wall temperature plays an important role on self-sustainment or reignition of the microcombustion in hypersonic flows. Since the assumption of single-step simple chemistry model is a major approximation of the simulation, the present results can be seen as a preliminary prediction for understanding the general trends of microcombustion phenomena.

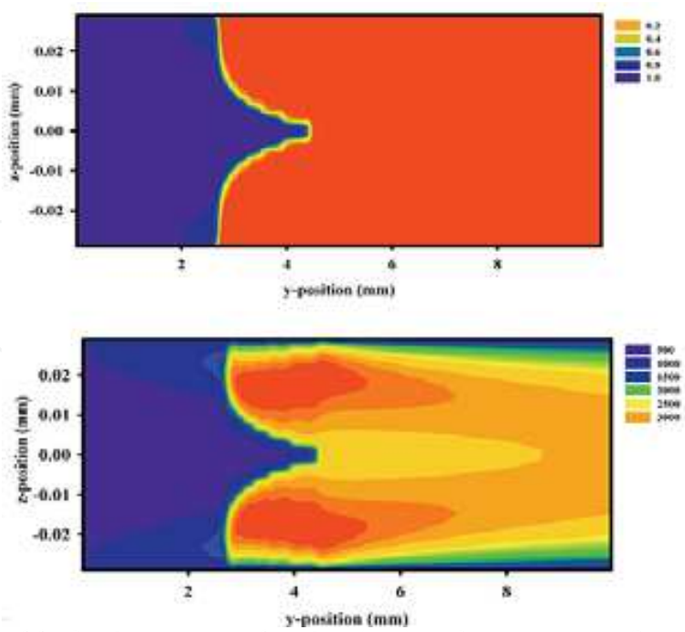

Fig. 4.5 Contours of fuel-mixture mass fraction (top) and temperature (bottom) for case 1

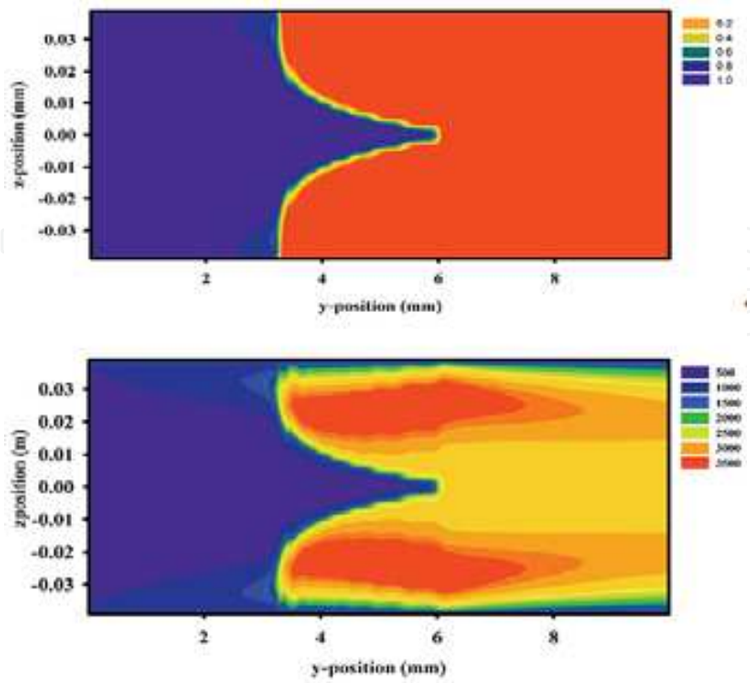

Fig. 4.6 Contours of fuel-mixture mass fraction (top) and temperature (bottom) for case 2

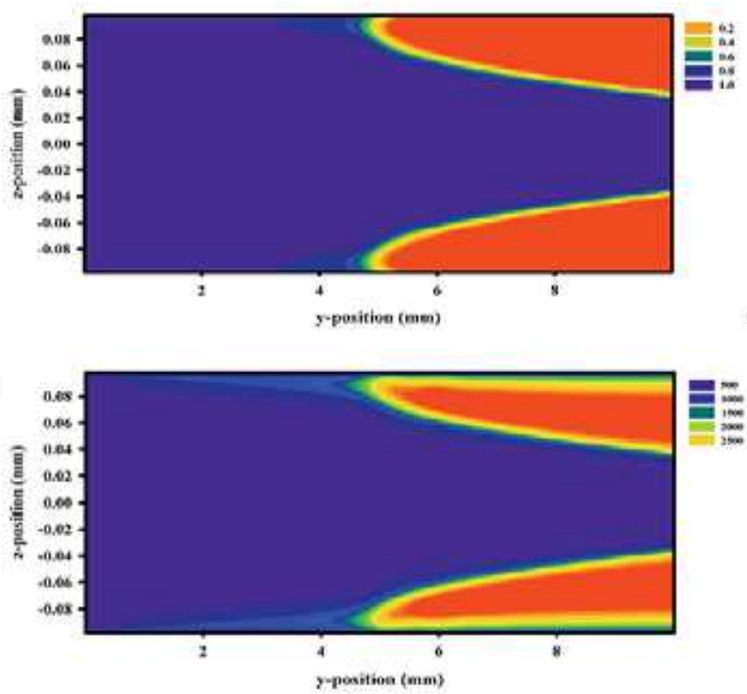

Fig. 4.7 Contours of fuel-mixture mass fraction (top) and temperature (bottom) for case 3

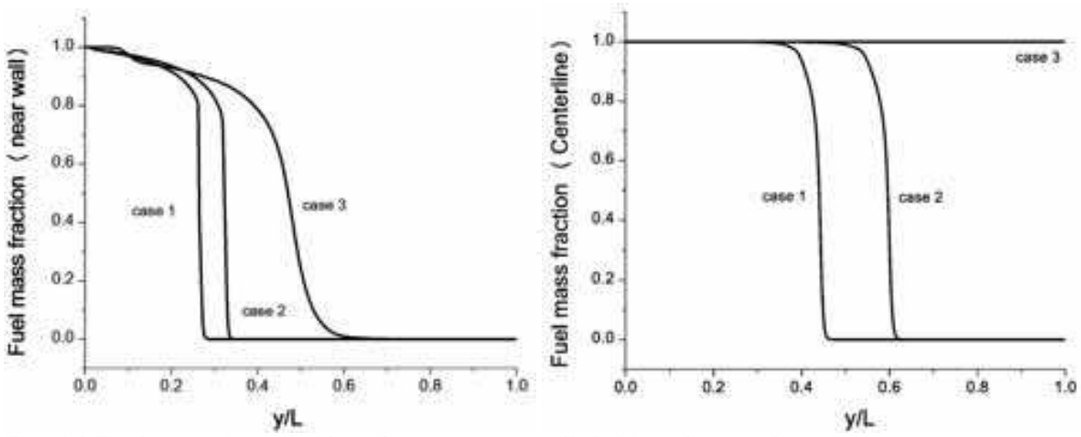

Fig. 4.8 Fuel mass fraction distribution near wall (left) and centerline

5. Shock-waves in Microscales

Thermal losses severely degrade the efficiency of miniaturized devices like internal combustion engines and gas turbines. In microscale devices shock waves can be exploited to produce shock-assisted (or shock-induced) combustion (Brouillette 2003). The behavior of conventional shock tubes at low pressure deviates from the ideal 1D gas dynamics theory. The properties of shock waves for low initial pressure were first examined by Duff, (1959). In general, shock tube flows are sensitive to boundary layer effects because they lead to flow non-uniformities, shock-wave attenuation and reduction in test time. Mirels, (1957) presented a methodology to compute the attenuation of shock waves by the method of characteristics. Later, Mirels, (1963, 1966) developed a theoretical model incorporating the influence of boundary layer on shock wave propagation. In microdimensions the shock tube behavior also suffers from strong deviation from the ideal case. Due to recent progress in the development of microdevices, several authors studied the characteristics of shock-wave propagation in mini/microchannels (Sun et al., 2001; Brouillette, 2003; Udagawa et al., 2007; Zeitoun and Burtschell, 2006; Parisse et al., 2008). Brouillette, (2003) proposed a 1D model to account for the scaling effects via molecular diffusion phenomena to analyse the generation and the propagation of shock waves. Zeitoun & Burtschel, (2006) numerically showed that the attenuation of the shock wave intensity is stronger for lower initial pressure or/and for smaller tube diameter. The effects of slip boundary conditions were found to be important. Zeitoun et al., (2007) also compared the prediction of shock wave propagation in the microtubes and microchannels using three different numerical approaches, namely DSMC method, BGK model and Navier-Stokes system of equations with slip models. In recent works of Mirshekari & Brouillette, (2009), a combined approach using 1D model and numerical simulations has been proposed to predict the performance of a microscale shock tubes with 3D effects incorporating source terms in conservation equations. It can be realized that at lower pressure ratios the shock wave tends to become nonexistent in microscale. In terms of applications, microscale shock tube material with lower thermal conductivity is recommended by Mirshekari & Brouillette, (2009) to achieve desired high temperature-jump. We carried out three demonstratives test-cases to show the effect of lowering the initial pressure (P_1) of driven-gas (argon) for a 1mm (L) by 10μm (H) channel

(case 1: 1atm, case 2: 0.5atm and case 3: 0.1atm). The pressure of the driver-gas (oxygen), P_4, has been calculated from the theoretical value which gives the pressure ratio (P_4/P_1) as function of the incident Mach number (M_s).

$$\frac{P_4}{P_1} = \frac{1 + \frac{2\gamma_1}{\gamma_1 + 1}\left(M_s^2 - 1\right)}{\left[1 - \frac{\gamma_4 - 1}{\gamma_4 + 1}\left(\frac{a_1}{a_4}\right)\left(M_s - \frac{1}{M_s}\right)\right]^{\frac{2\gamma_4}{\gamma_4 - 1}}} \tag{7}$$

where a_1 and a_4 are the speed of sound for driven-gas and driver-gas respectively.
M_s has been taken as 1.6 for the three test-cases. Owing to the symmetry of the problem only half of the physical domain has been simulated considering symmetry boundary conditions (on the top) and first-order slip boundary conditions (on the bottom). Based on Knudsen number criteria and previous studies (Zeitoun & Burtschel, 2006), the effect of thermal creep was neglected. Isothermal wall conditions (with a fixed wall temperature 300K) are imposed for all the considered cases. Unsteady computations have been carried out and the simulations have been stopped before the shock wave and the expansion fan reach the right and left boundaries of the computational domain.

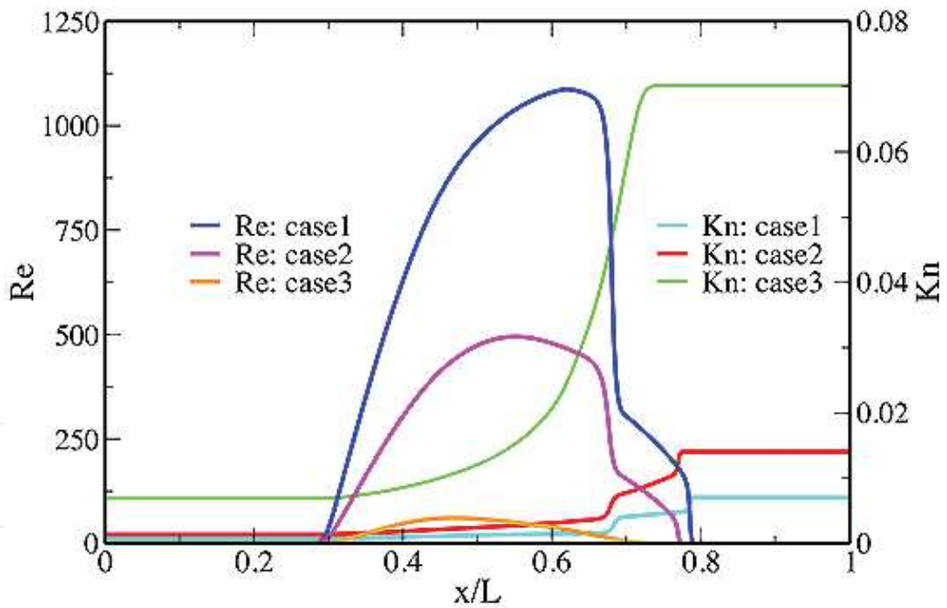

Fig. 5.1 Comparison of Reynolds number and Knudsen number

Reynolds and Knudsen numbers, based on centerline flow-field properties, have been shown in Figure 5.1. It is evident that Knudsen number is higher for driven-gas section having lower pressure, and Knudsen number is progressively higher from case 1 to case 3. Presence of dominant viscous effects can also be realized from lowest Reynolds number for case 3.

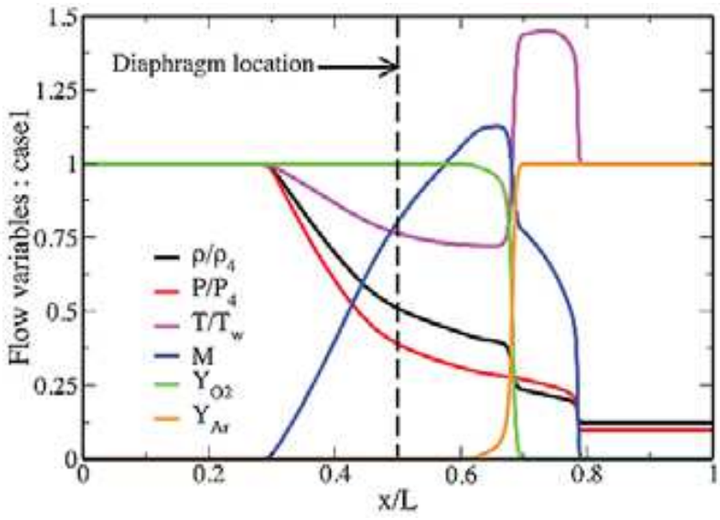

Fig. 5.2 Flow variables for case 1

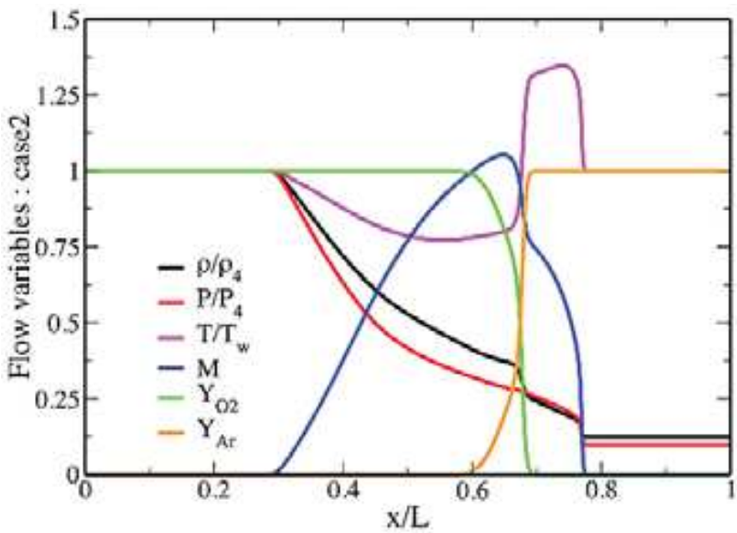

Fig. 5.3 Flow variables for case 2

Figs. 5.2-5.4 show the flow field parameters at non-dimensional time $\tau = ta_1/H = 20$. It can be seen that the strength of the shock gradually becomes weaker in cases from 1 to 3. The contact discontinuity location can be visualized from species mass fraction profile for each test case. Comparisons of dimensionless streamwise velocities (here, we used the speed of sound a_1 as a reference velocity) have been illustrated in Figure 5.5. The attenuation and retardation of shock propagation are clearly visible from this figure. Indeed for case 3, shock wave became almost nonexistent compared to the other two cases.

Finally, the shock location has been recorded and shown in Figure 5.6 for all cases. The ideal curve corresponds to the theoretical M_s = 1.6. It is evident that damping of shock propagation increases with the increase of Knudsen number associated with lower initial driven-gas pressure.

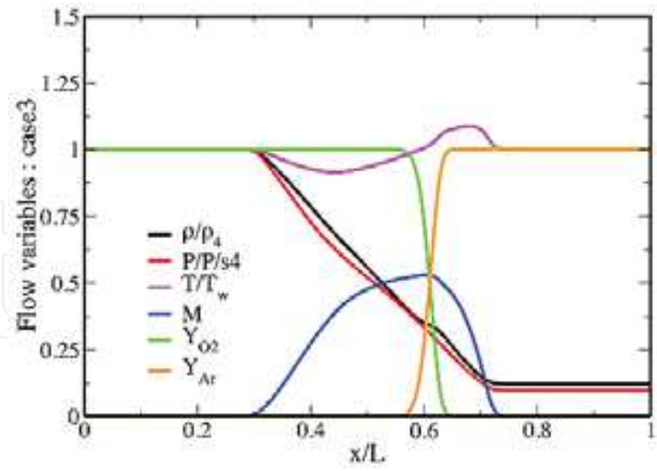

Fig. 5.4 Flow variables for case 3

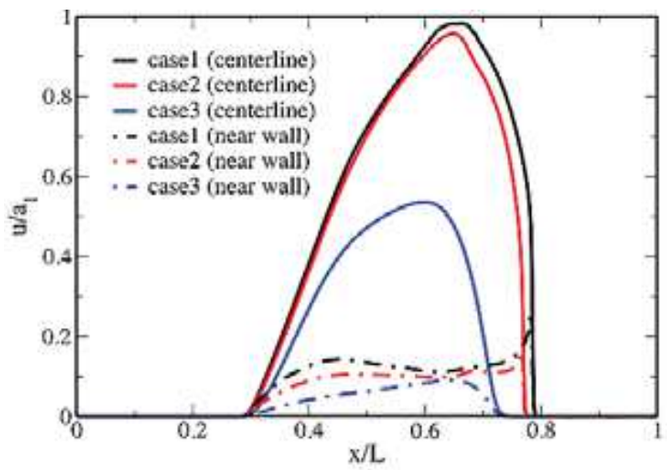

Fig. 5.5 Comparison of streamwise velocities

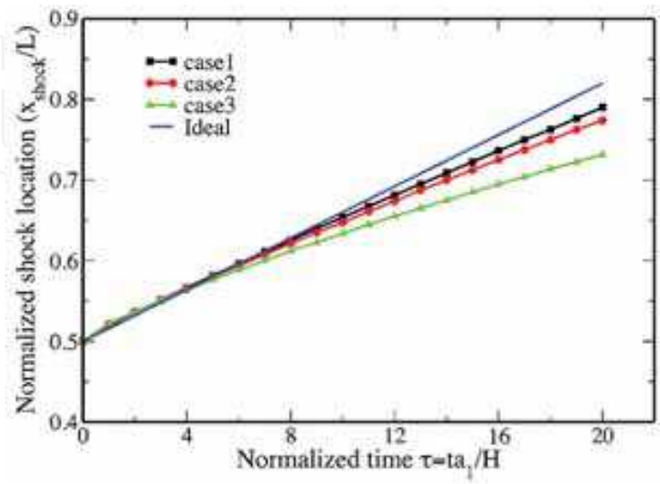

Fig. 5.6 Evolution of shock-position

6. Conclusions

In this chapter, we have provided a brief literature survey on compressible, reacting and non-reacting microscale gas flows including some of our recent numerical findings. The applicability of Navier-Stokes solutions with wall-slip models proved to be very cost-effective numerical approach for successful prediction of gas flows and thermal characteristics in microdevices. In particular, the validation of implemented first-order slip model has been achieved in solving various relevant benchmark problems. First, partially heated microchannel, resembling the classical Graetz problem, has been investigated with respect to the effect of Knudsen number as well as gas species. Then, high-speed supersonic and hypersonic flows with heat transfer in microchannel have been investigated. It has been found that the wall temperature jump is higher for higher inlet Mach numbers. Differences between conventional and microscale nozzle flows have been illustrated through different numerical simulations. Specifically, shock-free supersonic flow has been observed in micronozzles, contrary to conventional full-scale nozzles, and boundary-layer separation phenomenon has been found to be less pronounced in microscales. For the reacting cases, a specific solver has been developed for predicting the mechanism of flame acceleration and microcombustion in high-speed premixed stoichiometric air-acetylene mixture inside microchannels. The complex interactions among hydrodynamic process, shock structures and combustion have been predicted using a simplified single-step chemistry model. It can be concluded that microcombustion in high-speed flows can be achieved in suitably preheated stoichiometric premixed fuel-oxidizer. Furthermore, thermal loss is an important factor in high-speed microcombustion. In addition, in order to get better insights into the physics of shock-wave phenomena, attenuation of shock waves in microdimensions through both viscous and thermal effects has been reported.

One can notice that theoretical knowledge is presently more advanced for gas-flows than for liquid/two-phase flows in microchannels. However, there exists the need for precise experimental data both for steady and unsteady reacting and non-reacting microscale gas flows to definitely validate the choice of the best boundary model in the slip flow regime. Application of high-order slip models needs further intensive numerical investigations. Determination of the appropriate values of the accommodation coefficients also remains an open issue. Theoretical investigations relative to unsteady or thermally driven microflows would also need to be supported by smart experiments. Although the present two-dimensional studies reveal many important features of microscale flows and gaseous reactions, three-dimensional studies are required to get better insight into the physics of microflows. Incorporation of heat-loss mechanism through solid wall and detailed multi-step chemical reaction models, in case of reacting simulations, are also crucial aspects for more realistic and high-fidelity numerical predictions.

7. References

Alexeenko, A.A.; Levin, D. A.; Gimelshein, S. F.; Collins, R. J. & Markelov, G. N. (2002). Numerical simulation of high-temperature gas flows in a millimeter-scale thruster. *J. of Thermophysics & Heat Transfer*, 16, 1, 10-16

Arkilic, E.B.; Breuer, K.S. & Schmidt, M.A. (1994). Gaseous flow in microchannels. FED-Vol. 197, *Application of Microfabrication to Fluid Mechanics*, *ASME*, 57-66

Arkilic, E. B.; Breuer, K. S. & Schmidt, M. A. (1997a). Gaseous slip flow in long microchannels. *J. Microelectromech. Syst.*, 6,167–178

Arkilic, E.B.; Schmidt, M.A. & Breuer, K.S. (1997b). TMAC measurement in silicon micromachined channels. *Rarefied Gas Dynamics*, 20

Arkilic, E B.; Breuer, K. S. & Schmidt, M. A. (2001). Mass flow and tangential momentum accommodation in silicon micromachined channels. *J. Fluid Mech.*, 437, 29–43

Bayt, R. L.; Ayon, A.A. & Breuer, K. S. (1997). A performance evaluation of MEMS based micronozzle. *AIAA* 97-3169

Bayt, R. L. & Breuer, K. S. (1998). Viscous effects in supersonic MEMS-fabricated micronozzles. *Proceedings of 3rd ASME Microfluids Symposium.* Anaheim, CA

Bayt, R. L. (1999). Fabrication and testing of a MEMS based micropropulsion systems. *PhD thesis* MIT, Cambridge, MA

Beskok, A.; Trimmer, W. & Karniadakis, G. E. (1996). Rarefaction and compressibility effects in gas microflows, *J. Fluids Eng*., 118, 3, 448-456

Boyarko, G.A.; Sung, C. J. & Schneider, S. J. (2005). Catalyzed combustion of hydrogen–oxygen in platinum tubes for micro-propulsion applications. *Proceedings of the Combustion Institute*, 30, 2481–2488

Brouillette, M. (2003). Shock waves at microscales. *Shock Waves*, 13, 3–12

Celata, G. P. ; Cumo, M.; McPhail, S. J.; Tesfagabir, L. & Zummo, G. (2007). Experimental study on compressible flow in microtubes. *Int. J. Heat & Fluid Flow*, 28, 28-36

Chaudhuri, A.; Guha, C. & Dutta, T. K. (2006) Numerical study of micro-scale gas flow using finite volume method, *Journal of Physics Conference series*, 34, 291-297

Chaudhuri, A.; Guha, C. & Dutta, T. K. (2007a). Finite volume simulation of supersonic to hypersonic gas flow and heat transfer through microchannels, *Chem. Eng. Technol.,* 30,1, 41-45

Chaudhuri, A.; Guha, C. & Dutta, T. K. (2007b). Numerical study of fluid flow and heat transfer in partially heated microchannels using explicit finite volume method, *Chem. Eng. Technol.,* 30, 4, 425-430

Chaudhuri, A.; Guha, C. & Dutta, T. K. (2007c). Finite volume simulation of high speed combustion of premixed air-acetylene mixtures in a microchannel, *Chem. Eng. Technol.,* 30, 5, 615-620

Chaudhuri, A.; Guha, C. & Dutta, T. K. (2007d). Numerical study of flame acceleration in microchannel, *Proceedings of NSTI, Nanotech 2007, Santa Clara Convention Center*, Santa Clara, California, Vol. 3, 149-152, May 20-24, 2007

Chaudhuri, A.; Guha, C. & Dutta, T. K. (2008). Numerical study of microscale gas flow-separation using explicit finite volume method, *Proceedings of World Academy of Sciences, Engineering and Technology*, Vol. 36, 338-341, ISSN 2070-3740, December 2008

Chen, C. S. (2004). Numerical method for predicting three-dimensional steady compressible flow in long microchannels. *J. Micromech. Microeng*., 14, 1091–1100

Chen, K.; Winter, M. & Huang, R. F. (2005). Supersonic flow in miniature nozzles of planar configuration, *J. Micromech. Microeng*. 15, 1736–1744

Choi, S.B.; Barron, R.F. & Warrington, R.O. (1991). Fluid flow and heat transfer in microtubes. In Micro mechanical Sensors, Actuators, and Systems, *ASME Winter Annual meeting*, 123-133, Atlanta, GA

Colin, S.; Lalonde, P. & Caen, R. (2004). Validation of a second-order slip flow model in rectangular microchannels. *Heat Transfer Eng*., 25, 23–30

Colin, S. (2005). Rarefaction and compressibility effects on steady and transient gas flows in microchannels. *Microfluid Nanofluid*, 1, 268–279

Davy, H. (1817). Some researches on flame. *Transactions of the Royal Society of London*, 107, 45–76

Dongari, N.; Agrawal, A. & Agrawal, A . (2007). Analytical solution of gaseous slip flow in long microchannels. *Int. J. Heat & Mass Transfer*, 50, 3411–3421

Duff, R.E. (1959). Shock-tube performance at low initial pressure. *Phys. Fluids,* 2(2), 207–216

Ewart, T.; Perrier, P.; Graur, I. & Me´olans, J. G. (2007). Tangential momemtum accommodation in microtube. *Microfluid Nanofluid*, 3, 689–695

Federici, J.A. & Vlachos, D.G. (2008). A computational fluid dynamics study of propane/air microflame stability in a heat recirculation reactor. *Combustion and Flame,* 153, 258-269

Fukuda, M.; Koji, K. & Sakamoto, M. (1981). On quenching distance of mixtures of methane and hydrogen with air. *Bulletin of the JSME*, 24(193), 1192–1197

Gad-el-Hak, M. (1999). The fluid mechanics of microdevices-The freeman scholar lecture. *J. Fluids Eng*., 121, 5-33

Gamezo, V. N. & Oran, E. S. (2006). Flame acceleration in narrow channels: Application for micropropulsion in low gravity environment, *AIAA J*., 44, 329-336

Hammel, J. R. (2002). Development of an unstructured 3D DSMC/Particle-in-cell code and the simulation of microthruster flows. *MS Thesis,* Mech. Engg. Worcester Polytechnic Institute

Hao, P. F.; Ding, Y.; Yao, Z.; He, F. & Zhu, K. (2005). Size effect on gas flow in micro nozzles. *J. Micromech. Microeng*., 15, 2069–2073

Harley, J.C.; Huang, Y.; Bau, H.H. & Zemel, J.N. (1995). Gas flow in microchannels. *J. Fluid Mech.*, 284, 257-274

Jain, V. & Lin, C. X. (2006). Numerical modeling of three-dimensional compressible gas flow in microchannels. *J. Micromech. Microeng*., 16, 292–302

Janson, S. W.; Helvajian, H. & Breuer, K. (1999). MEMS, microengineering and aerospace systems. *AIAA* 99-3802

Jiang, G. & Shu, C. W. (1996). Efficient implementation of weighted ENO schemes, *J. Comp. Phys*., 126, 202-228

Karniadakis, G. E. & Beskok, A. (2002). *Microflows: fundamentals and simulation*. Springer, Berlin Heidelberg New York

Kivotides, D. (2007). Viscous microdetonation physics. *Physics Letters A*, 363, 458–467

Kolb, G. & Hessel, V. (2004). Micro-structured reactors for gas phase reactions. *Chemical Engineering Journal*, 98, 1–38

Kujawa, J.; Hitt, D.L. & Cretu, G. (2003). Numerical simulation of supersonic flow in MEMS nozzle geometries with heat loss*, AIAA Paper* 2003-3585

Le, M. & Hassan, I. (2006). Simulation of heat transfer in high speed microflows, *App. Thermal Eng*., 26, 2035-2044

Leach, T. T.; Cadou, C. P. & Jackson, G. S. (2006) Effect of structural conduction and heat loss on combustion in micro-channels. *Combustion Theory and Modelling*, 10, 1, 85–103

Lee, S. Y. K.; Wong, M. & Zohar, Y. (2001). Gas flow in microchannels with bends. *J. Micromech. Microeng*., 11, 635–644

Lee, D. H. & Kwon, S. (2002). Heat transfer and quenching analysis of combustion in a micro combustion vessel. *J. Micromech. Microeng*, 12, 670-676

Lee, D. H.; Park, D. E.; Yoon, J. B.; Kwon, S. & Yoon, E. (2002). Fabrication and test of a MEMS combustor and reciprocating device. *J. Micromech. Microeng.*, 12, 26–34

Lewis Jr., D. H. (2000). Digital micropropulsion. *Sensors and Actuators*, 80, 143–154 Lewis, B. & von Elbe, G. (1987). *Combustion, flames and explosions of gases*. Orlando, FL: Academic Press.

Li, Z. W.; Chou, S. K.; Shu, C.; Yang, W. M. & Xue, H. (2004). Predicting the temperature of a premixed flame in a microcombustor, *Journal of Applied Physics*, 96, 3524-3530

Li, Z.W.; Chou, S.K.; Shu, C.; Xue, H. & Yang, W.M. (2005a). Characteristics of premixed flame in microcombustors with different diameters. *Applied Thermal Engineering*, 25, 271–281

Li, Z. W.; Chou, S. K.; Shu, C. & Yang, W. M. (2005b). Effects of step height on wall temperature of a microcombustor. *J. Micromech. Microeng.*, 15, 207-212

Lin, C. X. & Gadepalli, V. V. V. (2008). A computational study of gas flow in a De-Laval micronozzle at different throat diameters. *Int. J. Numer. Meth. Fluids,* DOI: 10.1002/fld.1868

Linan, A. & Williams, F. A. (1993). *Fundamental aspects of combustion*. New York: Oxford University Press.

Liou, M. S. & Steffen Jr. C. J. (1993). A new flux splitting method. *J. of Computational Physics*, 107, 23-39

Liou, W. W. & Fang, L. Y. (2001). Heat transfer in microchannel devices using DSMC. *J. Microelectromech. Syst*., 2001, 10, 274–279

Liu, J.; Tai, Y. C. & Ho, C. M. (1995). MEMS for pressure distribution studies of gaseous flows in microchannels. *In: IEEE international conference on micro electro mechanical systems*. Amsterdam, Netherlands, 209–215

Liu, M.; Zhang, X.; Zhang, G. & Chen, Y. (2006). Study on micronozzle flow and propulsion performance using DSMC and continuum methods. *Acta Mechanica Sinica*, 22, 409–416

Maekawa, M. (1975). Flame quenching by rectangular channels as a function of channel length for methane-air mixture. *Combustion Science and Technology*, 11, 141–145.

Maruta, K.; Takeda, K.; Ahn, J.; Borer, K.; Sitzki, L.; Ronney, P. D. & Deutschmann, O. (2002). Extinction Limits of Catalytic Combustion in Microchannels. *Proceedings of the Combustion Institute*, 29, 957–963

Maurer, J.; Tabeling, P.; Joseph, P. & Willaime, H. (2003). Second-order slip laws in microchannels for helium and nitrogen. *Phys Fluids,* 15, 2613–2621

Miesse, C. M.; Masel, R. I.; Jensen, C. D.; Shannon, M. A & Short, M. (2004). Submillimeter-Scale Combustion. *AIChE Journal*, 50, 12, 3206-3214

Mirels, H. (1957). Attenuation in a shock tube due to unsteady-boundary -layer action. *Technical Report TN 1333*, National Advisory Committee for Aeronautics

Mirels, H. (1963) Test time in low-pressure shock tubes. *Phys. of Fluids*, 6, 9, 1201–1214

Mirels, H. (1966). Correlation formulas for laminar shock tube boundary layer. *Phys. Of Fluids,* 9, 7, 1265–1272

Mirshekari, G. & Brouillette, M. (2009). One-dimensional model for microscale shock tube flow. *Shock Waves*, 19, 25–38.

Moríñigo, J. A.; Quesada, J. H. & Requena, F. C. (2007). Slip-model performance for underexpanded micro-scale rocket nozzle flows. *J. of Thermal Science*, 16, 223-230

Norton, D. G.; Vlachos, D. G. (2003). Combustion characteristics and flame stability at the microscale: a CFD study of premixed methane/air mixtures. *Chemical Engineering Science*, 58, 4871 – 4882

Norton, D. G.; Vlachos, D. G. (2004). A CFD study of propane/air microflame stability. *Combustion and Flame*, 138, 97–107

Ott, J. D.; Oran, E. S. & Anderson, J. D. (2003). A mechanism for flame acceleration in narrow tubes, *AIAA J.*, 41, 1391-1396

Papautsky, I.; Ameel, T. & Frazier, A. B. (2001). A review of laminar single-phase flow in microchannels. *Proceedings of ASME Int. Mech. Eng. Cong. & Expo*. New York

Parisse, J. D.; Giordano, J.; Perrier, P.; Burtschell, Y. & Graur, I. A. (2008). Numerical investigation of micro shock waves generation. *Microfluid Nanofluid*, DOI 10.1007/s10404-008-0336-y

Pfahler, J.; Harley, J.; Bau, H. & Zemel, J. N. (1990). Gas and liquid transport in small channels. *Microstruct Sensors Actuators ASME*, 19, 149–157

Pong, K.C.; Ho, C.M. Liu J. & Tai, Y.C. (1994). Non-linear pressure distribution in uniform microchannels. *In Application of Microfabrication to Fluid Mechanics, ASME Winter Annual meeting*, 51-56, Chicago, Ill

Porodnov, B.T.; Suetin, P.E. ; Borisov, S.F. & Akinshin, V.D. (1974). Experimental investigation of rarefied gas flow in different channels. *J. of Fluid Mech.*, 64, 417-437

Raju, R.; Pandey, B.P. & Roy, S. (2002). Finite element model of fluid flow inside a micro-thruster, *Nano tech 2002-"At the edge of revolution", AIAA-2002-5733*, Houston, Texas

Raju, R. & Roy, S. (2005). Hydrodynamic study of high speed flow and heat transfer through a microchannel, *J. Thermophys. Heat Transfer*, 19, 106-113

Rawool, A. S.; Mitra, S. K. & Kandlikar, S. G. (2005). Numerical simulation of flow through microchannels with designed roughness. *Microfluid Nanofluid*, DOI 10.1007/s10404-005-0064-5

Reed, B. (2003). Decomposing solid micropropulsion nozzle performance issues. *AIAA 2003-672*

Rossi, C.; Rouhani, M. D. & Daniel, E. (2000). Prediction of the performance of a Si-micromachined microthruster by computing the subsonic gas flow inside the thruster, *Sensors and Actuators*, *Physical A*, 87, 96-104

Rossi, C.; Conto, T. D.; Esteve, D. & Larangot, B. (2001) . Design, fabrication and modelling of MEMS-based microthrusters for space Application. *Smart Mater. Struct*. 10 1156–1162

Rostami, A. A.; Mujumdar, A. S. & Saniei, N. (2002). Flow and heat transfer for gas flowing in microchannel: a review, *Heat and Mass Transfer*, 38, 359-367

San, O.; Bayraktar, I. & Bayraktar, T. (2009). Size and expansion ratio analysis of micro nozzle gas flow. *doi:10.1016/j.icheatmasstransfer.2009.01.021*

Schwarz, O.; Duong, P.Q.; Schäfer, G. & Schomäcker, R. (2009). Development of a microstructured reactor for heterogeneously catalyzed gas phase reactions: Part II. Reactor characterization and kinetic investigations *Chemical Engineering Journal*, 145, 429–435

Shaurya, S.; Armijo, A. D.; Masel, R. I. & Shannon, (2007). M. A. Flame dynamics in sub-millimetre combustors. *Int. J. Alternative Propulsion*, 1, 2/3, 325-338

Shih, J.C.; Ho, C.; Liu, J. & Tai, Y. (1996). Monatomic and polyatomic gas flow through uniform microchannels. *In Application of Microfabrication to Fluid Mechanics, ASME Winter Annual meeting*, 197-203, Atlanta, GA

Sreekanth, A. K. (1969). Slip flow through long circular tubes. *In: Trilling L, Wachman HY (eds) Proceedings of the 6th international symposium on rarefied gas dynamics.* Academic Press, New York, 667–680

Sun, M.; Ogawa, T. & Takayama, K. (2001). Shock propagation in narrow channels. In: Lu FK (ed) *Proceedings of 24th international symposium on shock waves*, 1320–1327

Udagawa, S.; Maeno, K.; Golubeva, I. & Garen, W. (2007). Interferometric signal measurement of shock waves and contact surfaces in small scale shock tube. *Proccedings of 26th international symposium on shock waves*, 2060

Wu, P. & Little, W.A. (1984). Measurement of the heat transfer characteristics of gas flow in fine channel heat exchanger used for microminiature refrigerators. *Cryogenics*, 24, 8, 15-420

Xu, B. & Ju, Y. (2004). Numerical modeling of the heterogeneous combustion in a microscale chemical reactor. *AIAA 2004-304*, 42nd AIAA Aerospace Sciences Meeting and Exhibit, Reno Hilton, Reno, Nevada

Xu, J. & Zhao, C. (2007). Two-dimensional numerical simulations of shock waves in micro convergent–divergent nozzles. *Int. J. of Heat & Mass Transfer*, 50, 2434–2438

Xue, H. & Chen, S. (2003). DSMC simulation of microscale backward-facing step flow. *Microscale Thermophysical Engineering*, 7, 69–86

Yan, F. & Farouk, B. (2002).Computation of fluid flow and heat transfer in ducts using the direct solution Monte Carlo method, *J. of Heat Transfer,* 124, 609-616

Yang, W.M.; Chou, S.K.; Shu, C.; Li, Z.W. & Xue, H. (2002). Combustion in micro-cylindrical combustors with and without a backward facing step. *Applied Thermal Engineering*, 22, 1777–1787

Yu, Z. T. F; Lee, Y; Wong, M. & Zohar, Y. (2005). Fluid flows in microchannels with cavities. *J. of Microelectromechanical Systems*, 14, 6, 1386 - 1398

Yuasa, S.; Oshimi, K.; Nose, H. & Tennichi, Y. (2005). Concept and combustion characteristics of ultra-micro combustors with premixed flame. *Proceedings of the Combustion Institute*, 30, 2455–2462

Zeitoun, D.E., Burtschel, Y. (2006). Navier–stokes computations in micro shock tubes. *Shock Waves,* 15, 241–246

Zeitoun, D. E.; Burtschell, Y. ; Graur, I.A. ; Ivanov, M. S.; Kudryavtsev, A. N. & Bondar, Y. A. (2007). Shock waves at microscalesn. *Proceedings of West-east high speed flow field Conference*, 19-22,Moscow, Russia

Recent Advances in Technologies

Edited by Maurizio A Strangio

ISBN 978-953-307-017-9

Hard cover, 636 pages

Publisher InTech

Published online 01, November, 2009

Published in print edition November, 2009

The techniques of computer modelling and simulation are increasingly important in many fields of science since they allow quantitative examination and evaluation of the most complex hypothesis. Furthermore, by taking advantage of the enormous amount of computational resources available on modern computers scientists are able to suggest scenarios and results that are more significant than ever. This book brings together recent work describing novel and advanced modelling and analysis techniques applied to many different research areas.

How to reference

In order to correctly reference this scholarly work, feel free to copy and paste the following:

A. Chaudhuri, A. Hadjadj, C. Guha and T. K. Dutta (2009). Numerical Simulations of Microscale Gas Flows: Continuum Approach, Recent Advances in Technologies, Maurizio A Strangio (Ed.), ISBN: 978-953-307-017-9, InTech, Available from: http://www.intechopen.com/books/recent-advances-in-technologies/numerical-simulations-of-microscale-gas-flows-continuum-approach

INTECH
open science | open minds

InTech Europe
University Campus STeP Ri
Slavka Krautzeka 83/A
51000 Rijeka, Croatia
Phone: +385 (51) 770 447
Fax: +385 (51) 686 166
www.intechopen.com

InTech China
Unit 405, Office Block, Hotel Equatorial Shanghai
No.65, Yan An Road (West), Shanghai, 200040, China
中国上海市延安西路65号上海国际贵都大饭店办公楼405单元
Phone: +86-21-62489820
Fax: +86-21-62489821

IntechOpen